Reconstruction by Site-Directed Mutagenesis of the Transition State for the Activation of Tyrosine by the Tyrosyl-tRNA Synthetase: A Mobile Loop Envelopes the Transition State in an Induced-Fit Mechanism†

Alan R. Fersht,*,‡ Jack W. Knill-Jones,‡ Hugues Bedouelle,§ and Greg Winter§

Department of Chemistry, Imperial College of Science and Technology, London SW7 2AY, U.K., and MRC Laboratory of Molecular Biology, MRC Centre, Hills Road, Cambridge CB2 2QH, U.K.

Received June 15, 1987; Revised Manuscript Received October 1, 1987

ABSTRACT: Site-directed mutagenesis of the tyrosyl-tRNA synthetase followed by kinetic studies has shown that residues which are distant from the active site of the free enzyme are brought into play as the structure of the enzyme changes during catalysis. Positively charged side chains which are in mobile loops of the enzyme envelope the negatively charged pyrophosphate moiety during the transition state for the formation of tyrosyl adenylate in an induced-fit mechanism. Residues Lys-82 and Arg-86, which are on one side of the rim of the binding site pocket, and Lys-230 and Lys-233, which are on the other side, have been mutated to alanine residues and also to asparagine or glutamine. The resultant mutants still form 1 mol of tyrosyl adenylate/mol of dimer but with rate constants up to 8000 times lower. Construction of difference energy diagrams reveals that all the residues specifically interact with the transition state for the reaction and with pyrophosphate in the E·Tyr-AMP·PP_i complex. Yet, the ϵ-NH_3^+ groups of Lys-230 and Lys-233 in the crystalline enzyme are at least 8 Å too far away to interact with the pyrophosphate moiety in the transition state at the same time as do Lys-82 and Arg-86. Binding of substrates must, therefore, induce a conformational change in the enzyme that brings these residues into range. Consistent with this proposal is the observation that all four residues are in flexible regions of the protein. The induced-fit mechanism allows access of substrates to the active site and enables the transition state to be completely surrounded by groups on the protein which would otherwise block entry.

The aminoacyl-tRNA synthetases catalyze the formation of aminoacyl-tRNA by first forming an enzyme-bound aminoacyl adenylate complex (eq 1, =activation) and then transferring the amino acid to tRNA (eq 2). The mechanism of activation

$$E + AA + ATP = E\cdot AA\text{-}AMP + PP_i \quad (1)$$

$$E\cdot AA\text{-}AMP + tRNA = AA\text{-}tRNA + E + AMP \quad (2)$$

has proved an enigma. Despite intensive work on the 20 different types of enzyme, there is no convincing evidence from classical kinetic experiments or protein chemistry for any uniquely important residues as used in conventional acid–base or covalent catalysis. Further, there is little convincing sequence homology between synthetases apart from the motif Cys-35...His-45...His-48 (numbered according to the tyrosyl-tRNA synthetase) noted first at the active site of the tyrosyl- and methionyl-tRNA synthetases (Barker & Winter, 1982). The initial crystal structures also failed to identify catalytic groups, but systematic site-directed mutagenesis has begun to unravel the catalytic mechanism (Winter et al., 1982). Residues that appear to interact with the substrates in the crystal structure of the enzyme-bound tyrosyl adenylate complex have been mutated. Residues that are nominally in the site for binding adenosine have been found to bind ATP not in the ground state (enzyme–tyrosine–ATP or enzyme–ATP complexes) but in the transition state and enzyme-bound tyrosyl adenylate complex (e.g., Cys-35 and His-48; Wells & Fersht, 1986; Fersht et al., 1986a). Mutagenesis of His-45 indicated that it was involved in binding the transition state of the reagents. Subsequent model building of the enzyme–transition-state complex revealed a binding site for the γ-phosphate of ATP between Thr-40 and His-45 in the transition state, which was confirmed by mutagenesis of Thr-40 (Leatherbarrow et al., 1985; Leatherbarrow & Fersht, 1987).

An important strategy for analyzing the results of mutation has been to determine the apparent contribution to the binding energy of the mutated side chain at each state of the reaction from difference energy diagrams (Wells & Fersht, 1986; Ho & Fersht, 1986). These are constructed by comparison of the free energy profiles of the reaction of wild-type and mutant enzymes as determined by measuring all the necessary rate and equilibrium constants in eq 3. Difference energy diagrams

$$E \underset{K_t}{\overset{Tyr}{\rightleftharpoons}} E\cdot Tyr \underset{K'_a}{\overset{ATP}{\rightleftharpoons}} E\cdot Tyr\cdot ATP \underset{k_{-3}}{\overset{k_3}{\rightleftharpoons}} E\cdot Tyr\text{-}AMP\cdot PP_i \underset{PP_i}{\overset{K_{PP}}{\rightleftharpoons}} E\cdot Tyr\text{-}AMP \quad (3)$$

show directly the effects of the mutation on the binding of each substrate, intermediate, and transition state. A spurious effect of a residue in the ATP site affecting the binding of tyrosine, for example, is immediately obvious. The combination of sensible difference energy diagrams, sensitive kinetic tests [e.g., the double-mutant test (Carter et al., 1984)], but especially the finding of linear free energy relationships (Fersht et al., 1986b, 1987) and X-ray crystallographic evidence (Brown et al., 1987) provides strong evidence that the results of these mutations reflect just the local effects of the change of side chain rather than any gross change in enzyme structure.

Beyond Direct Crystallographic Information. The kinetic methods have become even more important at the next stage of the investigation because we have now reached the limits of information presently available from protein crystallography on direct interactions between the enzyme and its substrates.

† This work was supported by the MRC of the U.K.

‡ Imperial College of Science and Technology.

§ MRC Centre.

0006-2960/88/0427-1581$01.50/0

The crystal structures of the free enzyme and of the enzyme–tyrosine complexes are those of a symmetrical dimer (Brick & Blow, 1987). But, it is known from solution studies that only 1 mol of tyrosine is bound per mole of dimer (Fersht, 1975) and that binding is accompanied by a change in the tryptophan fluorescence. Only 1 mol of tyrosyl adenylate is formed, and this is accompanied by a further similar change in fluorescence (Fersht et al., 1975). Substrate-induced conformational changes are clearly indicated, but their magnitude in structural terms is unknown. But, could these changes bring residues distant from the active site in the crystal structure into the mechanism? Clues came from a study in which most of the basic residues of the enzyme had been mutated to map out the tRNA binding site (Bedouelle & Winter, 1986). This revealed that several mutants (Lys → Asn-82, Arg → Gln-86, Lys → Asn-230, and Lys → Asn-233) were defective in activation of tyrosine. Lys-82 and Arg-86 are at one side of the entrance to the substrate binding pocket and Lys-230 and Lys-233 are at the opposite side. We have now characterized these mutants and a further set in which residues 82, 86, 230, and 233 have each been mutated to alanine.

Experimental Procedures

Materials

Restriction and other enzymes were obtained from Boehringer-Mannheim, chemicals from Sigma (London), and radiochemicals from Amersham International.

Methods

Production of Mutants. Mutants Lys → Asn-82, Arg → Gln-86, Lys → Asn-230, and Lys → Asn-233 were previously constructed (Bedouelle & Winter, 1986) on a derivative of the original M13mp93TyrS vector (Winter et al., 1982) altered in two ways in the TyrS gene: (i) a deletion of 900 bp to the 5′ side of the promoter; (ii) deletion of a premature terminator between the promoter and the start of translation [elements 2 and 3 of Waye and Winter (1986)]. This improves the yield of TyrTS about 3-fold in infected cells. For experimental details and the strain constructions used in the site-directed mutagenesis, see Carter et al. (1985): the mutagenic oligonucleotides (Bedouelle & Winter, 1986) were used in "double priming" with the strand selection primer SEL1 on M13mp93amIVTyrTS gene IV, transfecting the heteroduplex into competent *Escherichia coli* HB2154 with a lawn of HB2151. In the present study, mutant Lys → Ala-233 was constructed with the primer 5′-GCCGCTTTCCGTTG*C-*CCCGAATTTCGT-3′ without strand selection, transfecting the heteroduplex into competent BMH71-18*mut*L with a lawn of BMH71-18. Mutants Lys → Ala-82, Arg → Ala-86, Lys → Ala-230, and Glu → Ala-235 were constructed with primers 5′-GCTTTTTG*C*CCCGCTC-3′, 5′-TCAGCGTGG*C-*CTCGCTTT-3′, 5′-CCCGAATG*C*CGTGCCG-3′, and 5′-GCCGCTTG*CCGTTT-3′ in double priming with the strand selection primer SEL3 on M13B19TyrTS template. Heteroduplex was transfected into competent HB2155 with a lawn of HB2151. The coding sequence of the TyrTS gene (Winter et al., 1983) was checked with a family of sequencing primers (Wilkinson et al., 1984). An asterisk follows a mismatched base in the mutagenic primers.

Purification of Enzymes. Mutant enzymes were expressed in *E. coli* TG2 hosts [*rec*A form of TG1 (Gibson, 1984)] and purified to electrophoretic homogeneity by modification of existing procedures (Wilkinson et al., 1983). An overnight culture of *E. coli* TG2 in 2× TY medium (16 g of tryptone, 10 g of yeast extract, and 5 g of NaCl per liter) was diluted 100-fold into 5 mL of fresh medium and grown to early log phase ($A_{550} \sim 0.05$) before infecting with recombinant M13 at high multiplicity of infection (>100). Growth was continued at 37 °C for 1 h before being transferred to 500 mL of fresh, prewarmed medium and shaken overnight. The cells were harvested by centrifugation at 7000 rpm for 15 min, resuspended in a buffer containing 50 mM tris(hydroxymethyl)-aminomethane hydrochloride (Tris-HCl) (pH 7.8), 1 mM ethylenediaminetetraacetic acid (EDTA), 5 mM 2-mercaptoethanol, and 0.1 mM phenylmethanesulfonyl fluoride, and immediately lysed by sonication. The lysate was heated at 56 °C for 40 min to precipitate endogenous enzymes from *E. coli* and clarified by centrifugation at 15 000 rpm for 30 min. The protein precipitating at 70% saturating ammonium sulfate (0 °C) was dialyzed for 1.5–3 h at 4 °C against 50 mM potassium phosphate (pH 6.5), 1 mM EDTA, 0.1 mM phenylmethanesulfonyl fluoride, and 0.1 mM tetrasodium pyrophosphate (to remove any enzyme-bound tyrosyl adenylate). After further dialysis for 1.5–3 h against the same buffer minus tetrasodium pyrophosphate, the protein was applied to a 2 × 5 cm column containing DEAE-Trisacryl M equilibrated in the same buffer. The column was washed with the starting buffer and eluted with a gradient of 50–350 mM potassium phosphate (pH 6.5) containing 1 mM EDTA and 0.1 mM phenylmethanesulfonyl fluoride. The enzyme, which eluted at about 150 mM salt, was dialyzed against 20 mM Tris-HCl, 1 mM EDTA, and 0.1 mM phenylmethanesulfonyl fluoride before purification on a Pharmacia FPLC Mono Q column (Lowe et al., 1985).

Kinetic Procedures

All experiments were performed at 25 °C in a standard buffer containing 144 mM Tris-HCl (pH 7.78), 0.14 mM phenylmethanesulfonyl fluoride, and 10 mM $MgCl_2$. (ATP was added as the magnesium salt to maintain the free Mg^{2+} at 10 mM.)

Activation. The rate constants for the formation of enzyme-bound tyrosyl adenylate by all the mutants other than Glu → Ala-235 were sufficiently low that the reaction could be monitored by manual sampling and trapping E·Tyr-AMP on nitrocellulose disks. A solution of 144 mM Tris-HCl–10 mM $MgCl_2$ containing [^{14}C]Tyr (210 or 522 mCi/mmol) and yeast inorganic pyrophosphatase (0.005 unit/mL) of total volume 150 μL was incubated at 25 °C; 15–30 μL of enzyme (2–10 μM) in the same buffer was added to initiate the reaction. Experiments to determine the values of K_M for ATP were generally conducted at 40 μM tyrosine and those for determining the K_M for tyrosine at 10 mM ATP. Samples (20 μL) were periodically withdrawn and layered onto a nitrocellulose disk which was under mild suction. The disk was then washed with 5 mL of Tris-HCl–$MgCl_2$ buffer, dried under an infrared lamp, and suspended in scintillant, and the retained E·[^{14}C]Tyr-AMP was assayed by scintillation counting. The reactions followed first-order kinetics, and seven samples were taken over five half-lives. The reactions were followed to completion (>10 half-lives) to obtain end points.

Pyrophosphorolysis. A solution of enzyme-bound [^{14}C]-Tyr-AMP was obtained by incubating enzyme in a buffer at pH 6 [130 mM [bis(2-hydroxyethyl)amino]tris(hydroxymethyl)methane (Bis-Tris), 10 mM $MgCl_2$] in the presence of 25 μM [^{14}C]Tyr and 25 mM Mg-ATP. The E·Tyr-AMP complex was desalted on a Sephadex G-50 (medium) column (1 × 25 cm) with standard pH 7.78 buffer. The enzyme-bound aminoacyl adenylates were stored under liquid nitrogen. The rate constants for pyrophosphorolysis were sufficiently low that the reactions could be monitored by manual sampling as above.

Table I: Activation of Tyrosine by Tyrosyl-tRNA Synthetase[a]

enzyme	K_t (μM)	K'_a (mM)	k_3 (s^{-1})	k_3/K'_a (s^{-1} M^{-1})	k_{-3} (s^{-1})	K_{pp} (mM)	k_{-3}/K_{pp} (s^{-1} M^{-1})
wild type	12	4.7	38	8080	16.6	0.61	27 200
Lys → Ala-82	13	~40[b]	~2[b]	50			730
Lys → Asn-82	13	5.2	0.3	58	0.26	1.5	170
Arg → Ala-86	7.5	9.9	5.0×10^{-3}	0.51			1.2
Arg → Gln-86	4	3.5	4.2×10^{-3}	1.2	3.5×10^{-3}	2.5	1.4
Lys → Ala-230	23	4.9	0.39	80			130
Lys → Asn-230	19	3.4	2.6×10^{-2}	7.6			15
Lys → Ala-233	10.4			3.0			9.8
Lys → Asn-233	12			0.2			0.38

[a] All experiments conducted in the standard buffer at 25 °C and pH 7.78. K_t, the dissociation constant of the E·Tyr complex, was determined by equilibrium dialysis. K'_a, the dissociation constant of ATP from the E·ATP complex, k_3 and k_{-3}, the rate constants for the forward and reverse reaction, and K_{pp}, the dissociation constant of PP_i from the E·Tyr-AMP·PP_i complex, were determined from pre-steady-state kinetics. K_t for some mutants was also determined kinetically from the rate of activation at subsaturating conconcentrations of ATP, and the values were found to be in excellent agreement with those from equilibrium dialysis. The blank entries in the table occur where the values of K'_a and K_{pp} are too high (>50 M and >10 mM, respectively) to be determined. k_3 and k_{-3} are consequently inaccessible, but the ratios k_3/K'_a and k_{-3}/K_{pp} may still be determined with precision.

The reaction was initiated by the addition of tetrasodium pyrophosphate to a solution of 100–400 nM E·[^{14}C]Tyr-AMP in the standard buffer (both solutions having been incubated at 25 °C) to give a final volume of 130 μL.

Pyrophosphate Exchange Kinetics. These were performed for the mutant Glu → Ala-235 in the standard buffer (Wilkinson et al., 1983).

Binding of Tyrosine. This was determined by equilibrium dialysis (Fersht, 1975).

Analysis of Kinetics. The first-order rate constants for the hydrolysis of E·Tyr-AMP (k_h) are comparable in some cases to those for its formation (k_f, eq 3a). The observed rate

$$E \xrightarrow[\text{Tyr, ATP}]{k_f} \text{E·Tyr-AMP} + PP_i \xrightarrow{k_h} E + \text{Tyr} + \text{AMP} \quad (3a)$$

constant for the formation of E·Tyr-AMP k_{obsd} is given by

$$k_{obsd} = k_f + k_h \quad (4)$$

and the steady-state concentration of E·Tyr-AMP ([E·Tyr-AMP]$_{SS}$) by

$$[\text{E·Tyr-AMP}]_{SS} = [E]_0\{k_f/(k_f + k_h)\} \quad (5)$$

where $[E]_0$ is the total concentration of enzyme. [k_h is the sum of the rate constants for dissociation of the adenylate and direct hydrolysis (Wells et al., 1986).] $[E]_0$ may frequently be measured by [E·Tyr-AMP]$_{SS}$ at saturating concentrations of substrates. Alternatively, the enzyme was assayed by its A_{280} as we find that mutants are generally greater than 90% active on active site titration. Thus

$$k_f = k_{obsd}[\text{E·Tyr-AMP}]_{SS}/[E]_0 \quad (6)$$

For reactions which are too slow to follow to completion, the value of k_f may be calculated from the initial rate of formation of E·Tyr-AMP v_0, since

$$v_0 = k_f[E]_0 \quad (7)$$

(Inorganic pyrophosphatase is added to remove any pyrophosphate that is produced and would otherwise obscure the kinetics.)

Results

Choice of Mutations. The most conservative mutation should be made when conducting a mutational analysis of the role of side chains in catalysis, removing the minimal amount of side chain and minimizing the change in properties. Truncating lysine residues to asparagine, and arginines to glutamines, has the advantage of retaining some of the hydrophobic portion of the side chain and a polar end. This is ideal for a surface residue that has no other role than to present a polar function to water. However, mutation to asparagine and glutamine could give artifacts because polar groups are introduced that can make spurious interactions with substrates and within the enzyme. We have, accordingly, constructed a further set of mutants in which the side chains have been cut right back by mutation to alanine. As is seen below, there are significant differences between mutating to Ala and mutating to Asn in two examples.

Mutation Dramatically Alters Reaction Rates. Mutation of each of the four residues causes large decreases in the rate of formation of enzyme-bound tyrosyl adenylate without concomitant decreases in its stability: 1 mol of tyrosyl adenylate accumulates per mole of enzyme dimer with $t_{1/2}$ of many seconds to several minutes. This allows the direct measurement by pre-steady-state kinetics of the formation of enzyme-bound tyrosyl adenylate with manual sampling and likewise the pyrophosphorolysis rates of the enzyme-bound complexes (Table I). The availability of pre-steady-state measurements allows confident and accurate determination of the activity of debilitated mutants whose activity under steady-state conditions could be obscured by contaminants or revertants.

The effect of mutation on the energy levels of each of the intermediates is seen readily from the difference energy diagrams (Figure 1), constructed as described by Wells and Fersht (1986). We first deduce from the kinetics how residues 82, 86, 230, and 233 interact with the substrates, transition states, and intermediates and then correlate the interactions with the crystal structure.

Lys-230 and Lys-233. Mutation to either alanine or asparagine gives very similar results for each residue. In all cases, the energy levels of the E·Tyr and E·Tyr-AMP complexes are either virtually unaffected or only slightly altered whereas the energy levels of the transition-state and E·Tyr-AMP·PP_i complexes are considerably raised. The dissociation constant of magnesium pyrophosphate from the complex is raised above the solubility and so becomes immeasurably high. The binding of ATP to the E·Tyr complexes of mutants Ala-230 and Asn-230 is only slightly weakened. The direct interpretation of the difference energies is that Lys-233 binds strongly to ATP, the transition state, and pyrophosphate while Lys-230 appears to bind strongly to the transition state and pyrophosphate only.

Arg-86 and Lys-82. Both mutants of Arg-86 have relatively small changes in the binding of Tyr, ATP, and Tyr-AMP, but there is a large destabilization of the transition state. Interestingly, although k_{-3}/K_{pp} is reduced to a similar low value in both cases, the value of K_{pp} is increased from 0.61 mM for wild-type enzyme to 2.5 mM for Gln-86 and becomes >10 mM

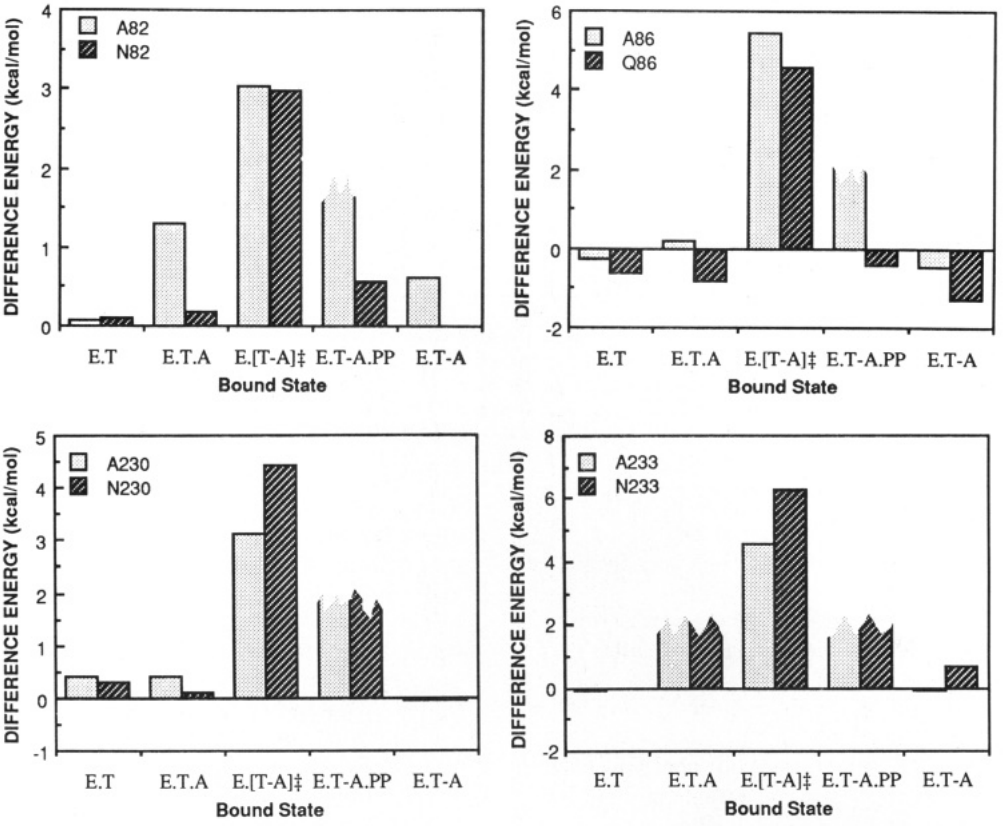

FIGURE 1: Difference energy diagrams (free energy of mutant complex − free energy of wild-type enzyme complex) for mutation of Lys → Ala-82 or Asn-82 (top right), Arg → Ala-86 or Gln-86 (top left), Lys → Ala-230 or Asn-230 (bottom left), and Lys → Ala-233 or Asn-233 (bottom right).

for Ala-86. The difference between Ala-86 and Gln-86 in binding pyrophosphate is what would be expected if Gln-86 is able to bind pyrophosphate but in a nonproductive mode. Classical nonproductive binding lowers individual values of k_{cat} and K_M in the Michaelis–Menten equation without altering their ratio. This illustrates the artifacts that can arise when side chains containing functional polar groups are used as replacements in mutagenesis. Arg-86 thus binds the transition state and pyrophosphate.

Mutation of Lys-82 is less clear cut. For both mutants, transition-state binding is weakened by 3 kcal/mol. Further for Ala-82, but not Asn-82, ATP binding is weakened significantly and pyrophosphate binding is greatly weakened. Since artifacts from spurious binding are likely to arise from the amide group of Asn, the results from Ala-82 probably reflect the binding properties of Lys-82. This appears to bind the transition state and pyrophosphate tightly and ATP weakly.

Discussion

The results show clearly that residues Lys-82, Arg-86, Lys-230, and Lys-233 interact with the transition state for the formation of tyrosyl adenylate and with pyrophosphate with relatively minor effects on the binding of tyrosine and tyrosyl adenylate (Figure 1). Further, Lys-82 interacts weakly and Lys-233 interacts strongly with ATP.

Correlation with Crystal Structure. The involvement of Lys-230 and Lys-233 in binding and catalysis is entirely unexpected from examination of the crystal structure. Residues 82, 86, 230, and 233 are on two exposed loops which have very high temperature factors (Brick & Blow, 1987). The temperature factor B is a measure of the disorder of atoms, that is, their equilibrium occupancy of different conformational states and/or their random motion between such states. The terminal guanidinium nitrogens of Arg-86 have B values of nearly 50 and so are on the borderline of being visible in the electron density map. The side chains of Lys-230 and Lys-233 are so mobile that they are not observable in the map. The long side chains of lysine residues are frequently mobile on the surface of proteins, and so it is not uncommon for the positions of the ϵ-NH_3^+ groups to be indeterminate. However, a plot of the average value of B for the peptide C and N, and the C_α of each residue (Figure 2), which gives a measure of the displacement of the backbone from its mean position, reveals that residues Lys-82 and Arg-86 are in a region of high mobility (residues 81–89, peaking at Arg-86). Lys-230 and Lys-233 are in an extended stretch of mobile backbone from residue 222 to residue 238, with exceptional mobility (residues 230–237, peaking at Glu-235).

Irrespective of the uncertainty in the positions of Lys-230 and -233, it is clear that there are side chains too far from the substrates for direct interaction without considerably movement of the loop. The α-carbon atoms of lysines-230 and -233 are 16–17 Å from the α-phosphate of tyrosyl adenylate. Building the side chains of the lysines in the most extended conformation possible, pointing toward the model of the transition state, does not allow direct contact: the closest distance of approach of the ϵ-NH_3^+ groups of either Lys-230 or Lys-233 is about 8 Å from an oxygen ion of the γ-phosphate, and they are further away from the α- and β-phosphates. These distances cannot be sensibly shortened by moving the pyrophosphate moiety of ATP toward Lys-230 and Lys-233 for two reasons. First, we know the position of the γ-phosphate in the transition state with some certainty from the earlier studies. Second, movement toward Lys-230 and Lys-233 would draw the phosphate groups away from Lys-82 and Arg-86—the pyrophosphate moiety cannot bind simultaneously to Lys-82 and Arg-86 on one side and Lys-230 and Lys-233 on the other.

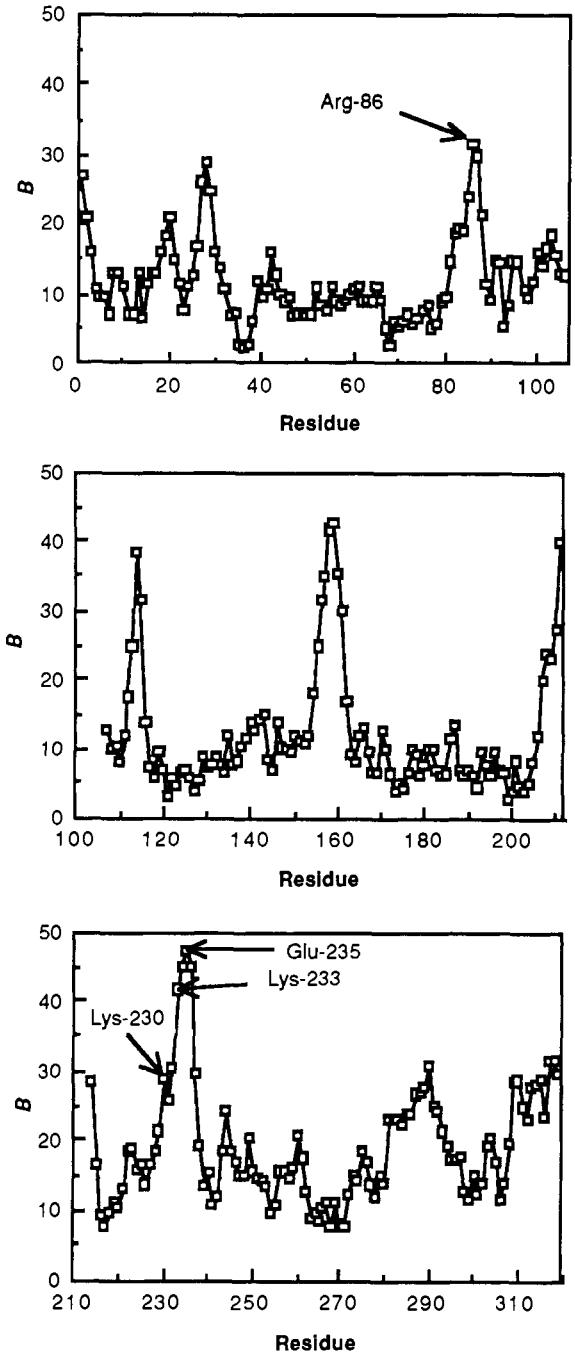

FIGURE 2: Crystallographic temperature factors for main chain. *B* values averaged for backbone C, N, and C_α taken from Brick and Blow (1987) and their unpublished data.

The position of Lys-82 is the clearest from crystallographic studies. Lys-82 in the E·Tyr-AMP complex appears to be coordinated to the α-phosphate of Tyr-AMP via a hydrogen-bonded bridging water molecule between the ϵ-NH_3^+ group and an oxygen atom (Brick & Blow, 1987). (This explains why the binding of Tyr-AMP is weakened on mutation to Ala-82.) The ϵ-NH_3^+ group of Lys-82 is about 3 Å from an oxygen atom of the β-phosphate in the model of the transition state. The guanidinium group of Arg-86 can be placed reasonably close to the β- and γ-phosphates in the modeled transition-state complex, at about 3 Å from an oxygen ion of the γ-phosphate and 3–4 Å from an oxygen ion of the β-phosphate. [It is worth noting that the transition state for the reaction was modeled originally into an earlier, less-refined, model of the enzyme in which the positions of Lys-82 and Arg-86 were not known because of their high temperature factors (Leatherbarrow et al., 1985). The proximity between the transition state and the two residues was found when the coordinates of the transition state were transferred to the refined structure (Brick & Blow, 1987) without any adjustment (R. J. Leatherbarrow, unpublished results).]

It is extremely unlikely that the interactions with Lys-230 and Lys-233 could arise from long-range electrostatic effects: such effects would not have the observed specificity for the transition state compared with ATP, and the experimental energies are far higher than for electrostatic effects recently measured in the active site of subtilisin (Russell et al., 1987).

Mechanistic Interpretation. The four residues must interact with ATP, the transition state, and pyrophosphate by the enzyme wrapping itself around the pyrophosphate moiety; that is, there is an induced-fit mechanism. The minimal reaction scheme is that ATP binds to the enzyme–tyrosine complex and draws in Lys-82 and Lys-233 (Figure 3). At that state, interactions are not made with Arg-86 and Lys-230 (this study) and also not with Cys-35, His-48 Thr-40, His-45, and Thr-51 (Wells & Fersht, 1986; Ho & Fersht, 1986). Strong interactions are made, however, between these residues and the transition state (Figure 3). Strong interactions are also made between the pyrophosphate and Thr-40, His-45, Lys-82, Arg-86, Lys-230, and Lys-233 in the E·Tyr-AMP·PP_i complex. In the E·Tyr-AMP complex, Lys-230 and Lys-233 move back to their positions in free enzyme, Arg-86 presumably also moves, and Lys-82 binds to the α-phosphate via a water molecule.

Likelihood of Additional Intermediate between Ground State and Transition State. It is expected from chemical reasoning that there is an intermediate between the E·Tyr·ATP complex and the transition state. It seems unlikely from the principle of least motion that the large change in enzyme structure on forming the transition state and the formation of the chemical bond between tyrosine and ATP would occur simultaneously. It is more likely that there is a high-energy intermediate between E·Tyr·ATP and E[Tyr-ATP]‡ in which the structure of the enzyme and the interactions between it and the substrate resemble those of the transition state (eq 8). The ground state or "open" complex does not make the

$$\text{E·Tyr·ATP}_{(\text{open})} \rightleftarrows \text{E·Tyr·ATP}_{(\text{closed})} \rightleftarrows \text{E[Tyr-ATP]}^\ddagger \quad (8)$$

energetically favorable hydrogen bonds/salt bridges between it and ATP. These are formed in the high-energy or "closed" complex, and their energies partly offset the energy that has it to be overcome to cause the conformational changes and distortions in the enzyme (Figure 4). The existence of the open complex would also explain why Cys-35 does not make a bond with ATP in the E·Tyr·ATP complex: it does not bind until the closed complex is reached.

Missing from the reaction scheme is the Mg^{2+} ion: the substrates for the reaction are Mg·ATP in the formation of E·Tyr-AMP and Mg·PP_i in its pyrophosphorolysis. Now that it has been demonstrated that mobile loops bring previously unsuspected side chains into play, we have begun investigating further residues in those regions. We have now found that Glu-235 is involved in the binding of ATP. Mutation of Glu → Ala-235 weakens the binding of ATP to the enzyme so that the dissociation constant becomes immeasurably high (>10 times the value for wild-type enzyme; J. W. Knill-Jones and A. R. Fersht, unpublished data) and raises the energy of the transition state by 1.8 kcal/mol. Glu-235 could well be involved in binding the coordinated magnesium ion in the E·Tyr·ATP complexes and in the transition state. The involvement of Glu-235 in binding is yet more evidence for the catalytic role of the mobile loop, and the binding energy be-

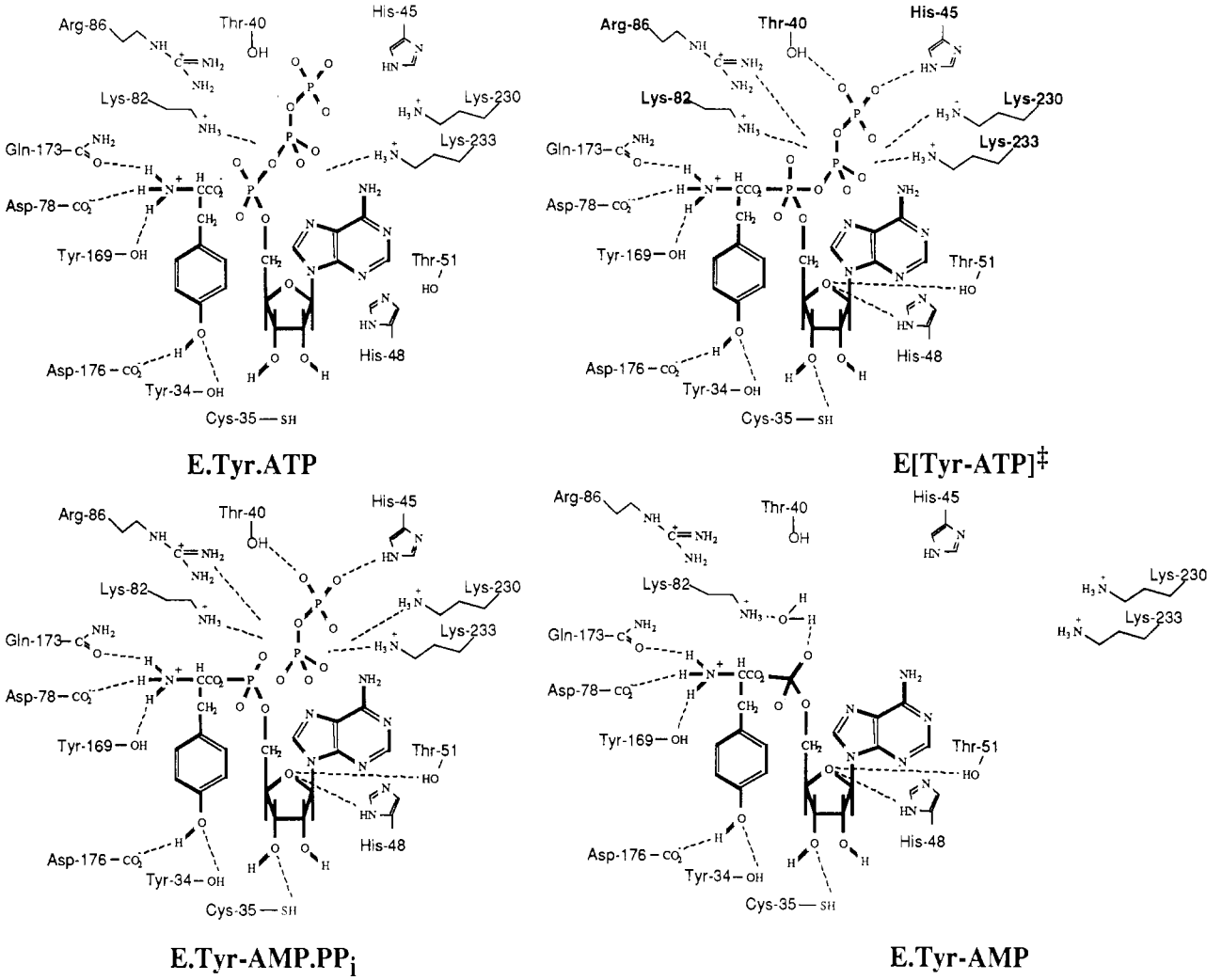

FIGURE 3: Binding events during the activation of tyrosine. (Top left) Ground-state E·Tyr·ATP complex: ATP binds to Lys-82 and Lys-233 and has insignificant binding energy with Cys-35, Thr-40, His-45, His-48, Thr-51, Lys-82, Arg-86, and Lys-230. (Top right) Transition-state complex: the charged and other groups interact with the pyrophosphate moiety of ATP and its ribose ring. (Bottom left) E·Tyr-AMP·PP_i complex: the groups still interact with the intermediate. (Bottom right) E·Tyr-AMP complex: the Lys-230/233 loop moves away from the adenylate after dissociation of PP_i, and Lys-82 binds to the α-phosphate of Tyr-AMP via a bridging water molecule (Brick & Blow, 1987).

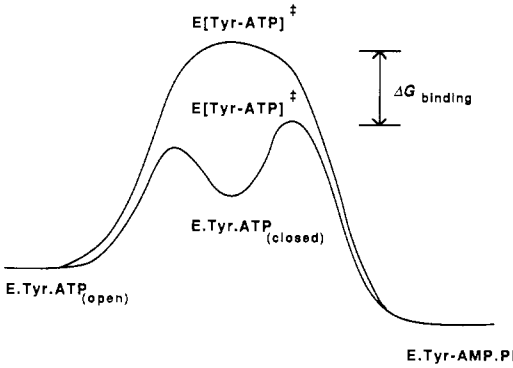

FIGURE 4: Free energy scheme for induced-fit process. (Upper curve) Hypothetical energy profile for formation of transition state in the absence of binding energy with enzyme. (Lower curve) Energy profile using binding energy, assuming the intermediacy of a high-energy conformation of ATP (E·Tyr·ATP_{closed}) which resembles the structure of the transition state that is stabilized by interactions with the enzyme. The activation energy is lowered by $\Delta G_{binding}$, the interaction energy of the transition state with the enzyme, compared with that in the E·Tyr·ATP_{open} complex.

tween Glu-235 and ATP provides additional binding energy for moving the loop to the substrate.

Why the Induced Fit? An enzyme catalyzes a reaction by specifically binding the transition state of the reaction. But, here the free enzyme is not complementary in structure to the transition state but has to be distorted. Distortion of the structure of the enzyme in the transition state costs energy and so is deleterious to catalysis. The enzyme is faced with two problems, however: that of surrounding the transition state with the necessary charged groups to stabilize it and also of allowing substrates access to the active site. The compromise is to have an open active site with binding groups in flexible regions of the protein and to use some of the binding energy of the substrate to distort the enzyme on binding.

Magnitude of Transition-State Stabilization. The energies in the difference energy diagrams are equal to $-\Delta\Delta G_{app}$, the change in free energy between wild-type and mutant enzymes from one state to the next along the reaction pathway described in the accompanying paper (Fersht, 1988). It appears at first sight from the difference energy diagram (Figure 1) that the four residues are stabilizing the transition state by some 15–18 kcal/mol. This would be in addition to the 8 or 9 kcal/mol seen in difference energy diagrams for mutation of Thr-40 and His-45 (Leatherbarrow et al., 1985; Leatherbarrow & Fersht, 1987). The sum of these values is too high to represent stabilization of the transition state as they would give a rate enhancement of 10^{17} or greater. The discrepancy could be for two reasons. First, additivity could simply break down for multiple substitutions. Second, although $\Delta\Delta G_{app}$ is generally

a reliable measure of changes in binding energy between the enzyme and substrate and the stabilization of one state relative to a previous one, there is an important exception. This is when groups in the ES complex shed their hydrogen bonds with water to form bonds with each other (Fersht, 1988). As emphasized in the accompanying paper (Fersht, 1988), deletion of a hydrogen-bond donor to a charged group will considerably overestimate the stabilization energy. This could well be the case here.

ACKNOWLEDGMENTS

We thank Professor David Blow and Dr. Peter Brick for continual access to the coordinates of the tyrosyl-tRNA synthetase during its refinement and Paul Deer and Peter Jones for technical assistance.

REFERENCES

Barker, D. G., & Winter, G. (1982) *FEBS Lett. 145*, 191–193.
Bedouelle, H., & Winter, G. (1986) *Nature (London) 320*, 371–373.
Brick, P., & Blow, D. M. (1987) *J. Mol. Biol. 194*, 287–297.
Brown, K. A., Brick, P., & Blow, D. M. (1987) *Nature (London) 326*, 416–418.
Carter, P. J., Winter, G., Wilkinson, A. J. & Fersht, A. R. (1984) *Cell (Cambridge, Mass.) 38*, 834–840.
Carter, P., Bedouelle, H., & Winter, G. (1985) *Nucleic Acids Res. 13*, 4431–4443.
Fersht, A. R. (1975) *Biochemistry 14*, 5–12.
Fersht, A. R. (1988) *Biochemistry* (preceding paper in this issue).
Fersht, A. R., Mulvey, R. S., & Koch, G. L. E. (1975) *Biochemistry 14*, 13–18.
Fersht, A. R., Wells, T. N. C., & Leatherbarrow, R. J. (1986a) *Trends Biochem. Sci. (Pers. Ed.) 11*, 321–325.
Fersht, A. R., Wells, T. N. C., & Leatherbarrow, R. J. (1986b) *Nature (London) 322*, 284–286.
Fersht, A. R., Leatherbarrow, R. J., & Wells, T. N. C. (1987) *Biochemistry 26*, 6030–6038.
Gibson, T. (1984) Ph.D. Thesis, University of Cambridge, U.K.
Ho, C., & Fersht, A. R. (1986) *Biochemistry 25*, 1891–1897.
Leatherbarrow, R. J., & Fersht, A. R. (1987) *Biochemistry 26*, 8524–8528.
Leatherbarrow, R. J., Fersht, A. R., & Winter, G. (1985) *Proc. Natl. Acad. Sci. U.S.A. 82*, 7840–7844.
Lowe, D. M., Fersht, A. R., Wilkinson, A. J., Carter, P., & Winter, G. (1985) *Biochemistry 24*, 5106–5109.
Russell, A. J., Thomas, P., & Fersht, A. R. (1987) *J. Mol. Biol. 193*, 803–813.
Waye, M. M. Y., & Winter, G. (1986) *Eur. J. Biochem. 158*, 505–510.
Wells, T. N. C., & Fersht, A. R. (1986) *Biochemistry 25*, 1881–1886.
Wells, T. N. C., Ho, C., & Fersht, A. R. (1986) *Biochemistry 25*, 6603–6608.
Wilkinson, A. J., Fersht, A. R., Blow, D. M., & Winter, G. (1983) *Biochemistry 22*, 3581–3586.
Wilkinson, A. J., Fersht, A. R., Blow, D. M., Carter, P., & Winter, G. (1984) *Nature (London) 307*, 187–188.
Winter, G., Fersht, A. R., Wilkinson, A. J., Zoller, M., & Smith, M. (1982) *Nature (London) 299*, 756–758.
Winter, G., Koch, G. L. E., Hartley, B. S., & Barker, D. G. (1983) *Eur. J. Biochem. 132*, 383–387.

Specific Labeling of the Essential Cysteine Residue of L-Methionine γ-Lyase with a Cofactor Analogue, *N*-(Bromoacetyl)pyridoxamine Phosphate†

Toru Nakayama, Nobuyoshi Esaki, Hidehiko Tanaka, and Kenji Soda*
Institute for Chemical Research, Kyoto University, Uji, Kyoto-Fu 611, Japan
Received June 22, 1987; Revised Manuscript Received September 3, 1987

ABSTRACT: L-Methionine γ-lyase from *Pseudomonas putida* is composed of four identical polypeptide chains and contains four cysteinyl residues per subunit. We have found one of them catalytically essential by its specific cyanylation with 2-nitro-5-thiocyanobenzoic acid. We have shown its essentiality also with *N*-(bromoacetyl)pyridoxamine 5′-phosphate (BAPMP), which is a cofactor analogue and also an affinity-labeling agent. The kinetic data show that the apoenzyme forms a binary complex with BAPMP prior to covalent binding. The stoichiometry of inactivation was 1 mol of BAPMP per subunit. We have shown that the cysteine residue modified with BAPMP is identical with that labeled specifically with [^{14}C]iodoacetic acid. The amino acid sequences of the peptides containing the essential cysteine residue and the lysine residue to which pyridoxal 5′-phosphate is bound were determined by automated Edman degradation.

L-Methionine γ-lyase (EC 4.4.1.11) is a pyridoxal-P[1] enzyme that catalyzes the α,γ-elimination of L-methionine to α-ketobutyrate, methanethiol, and NH_3. We have purified the enzyme from *Pseudomonas putida* and characterized it (Esaki et al. 1979, 1984, 1985; Nakayama et al., 1984). We have studied the mechanism of inactivation of the enzyme by a suicide substrate, L-propargylglycine, as well and shown that a nucleophilic amino acid residue located at the active site is modified with L-propargylglycine (Johnston et al., 1979). The presence of an essential cysteine residue of the enzyme was

† This work was supported in part by special coordination funds of the Ministry of Agriculture, Forestry and Fisheries of Japan.

[1] Abbreviations: pyridoxal-P, pyridoxal 5′-phosphate; BAPM, *N*-(bromoacetyl)pyridoxamine; BAPMP, *N*-(bromoacetyl)pyridoxamine 5′-phosphate; NTCB, 2-nitro-5-thiocyanobenzoic acid; DTT, dithiothreitol; DTNB, 5,5′-dithiobis(2-nitrobenzoic acid); EDTA, ethylenediaminetetraacetate; HPLC, high-performance liquid chromatography; PTH, phenylthiohydantoin; Tris-HCl, tris(hydroxymethyl)aminomethane hydrochloride.

0006-2960/88/0427-1587$01.50/0